Faraday Discussions

RSC Publishing

Cite this: *Faraday Discuss.*, 2013, **165**, 473

PAPER

View Article Online
View Journal | View Issue

Brown carbon formation from ketoaldehydes of biogenic monoterpenes†

Tran B. Nguyen,‡*[a] Alexander Laskin,[b] Julia Laskin[c] and Sergey A. Nizkorodov[a]

Received 10th March 2013, Accepted 10th April 2013
DOI: 10.1039/c3fd00036b

Sources and chemical composition of brown carbon are poorly understood, and even less is known about the mechanisms of its atmospheric transformations. This work presents molecular-level investigations of the reactive compound ketolimononaldehyde (KLA, $C_9H_{14}O_3$), a second-generation ozonolysis product of limonene ($C_{10}H_{16}$), as a potent brown carbon precursor in secondary organic aerosol (SOA) through its reactions with reduced nitrogen compounds, such as ammonium ion (NH_4^+), ammonia, and amino acids. The reactions of synthesized and purified KLA with NH_4^+ and glycine resulted in the formation of chromophores nearly identical in spectral properties and formation rates to those found in similarly-aged limonene/O_3 SOA. Similar chemical reaction processes of limononaldehyde (LA, $C_{10}H_{16}O_2$) and pinonaldehyde (PA, $C_{10}H_{16}O_2$), the first-generation ozonolysis products of limonene and α-pinene, respectively, were also studied, but the resulting products did not exhibit the light absorption properties of brown carbon, suggesting that the unique molecular structure of KLA produces visible-light-absorbing compounds. The KLA/NH_4^+ and KLA/GLY reactions produce water-soluble, hydrolysis-resilient chromophores with high mass absorption coefficients (MAC = 2000–4000 $cm^2\ g^{-1}$) at $\lambda \sim 500$ nm, precisely at the maximum of the solar emission spectrum. Liquid chromatography was used to isolate the light-absorbing fraction, and UV-Vis, FTIR, NMR and high-resolution mass spectrometry (HR-MS) techniques were

[a]*Department of Chemistry, University of California, Irvine, California, USA 92697. E-mail: tbn@calech.edu; Tel: +1-626-395-8650*

[b]*Environmental Molecular Sciences Laboratory, Pacific Northwest National Laboratory, Richland, Washington, USA 99352*

[c]*Physical Sciences Division, Pacific Northwest National Laboratory, Richland, Washington, USA 99352*

† Electronic supplementary information (ESI) available: Table S1 – NMR data for identification of PA, LA, and KLA; Fig. S1 – proton NMR spectra of LA, KLA, and PA confirming their purity; Fig. S2 – LC-UVIS separation of the C_{500} fraction; Fig. S3 – control experiment with evaporation of KLA alone with reduced nitrogen compounds added; Fig. S4 – comparison of the rates of aging of KLA and limonene SOA by gaseous ammonia; Fig. S5 – proton NMR spectra of the C_{500} fraction in D_2O and in H_2O; Fig. S6 – absorption spectra recoded by the PDA detector at different elution times; Fig. S7 – graphical representation of the compounds detected by HR-MS; Scheme S1 – reactions of KLA leading to low DBE compounds and supporting references. See DOI: 10.1039/c3fd00036b

‡ Currently at: Division of Geological and Planetary Sciences, California Institute of Technology, Pasadena, CA 91125.

used to investigate the structures and chemical properties of the light-absorbing compounds. The KLA browning reaction generates a diverse mixture of light-absorbing compounds, with the majority of the observable products containing 1–4 units of KLA and 0–2 nitrogen atoms. Based on the HR-MS product distribution, conjugated aldol condensates, secondary imines (Schiff bases), and N-heterocycles like pyrroles may contribute in varying degree to the light-absorbing properties of the KLA brown carbon. The results of this study demonstrate the high degree of selectivity of organic compound structures on the light-absorbing properties of SOA.

Introduction

Atmospheric aerosols scatter and absorb solar radiation; however, the magnitude and sign of their direct climate forcing remain uncertain.[1] Most climate models assume primary and secondary organic aerosols (POA and SOA) have only scattering components, resulting in negative climate forcing. However, the presence of black carbon and brown carbon[2] compounds in organic aerosols may significantly alter their climate forcing. While it is well-accepted that the dominant sources of black carbon are primary combustion emissions, the sources of brown carbon are not well-understood. Brown carbon can be directly emitted from combustion sources[2–4] as part of POA or created by reactions in the atmosphere, such as in the formation or aging of SOA. This *secondary brown carbon* can be formed from multiple precursors and a variety of reaction pathways, *e.g.*, the reactions of 1,2-dicarbonyls with ammonium (NH_4^+) salts,[5–10] the aqueous photooxidation of hydroxyacids,[11–13] the acid-catalysed condensation of volatile aldehydes,[14–21] and the nitration of aromatic compounds.[22–24]

Brown carbon formation has also been observed in the reaction of NH_4^+(aq), amino acids (aq), and NH_3(g) with SOA derived from the ozonolysis of limonene ($C_{10}H_{16}$).[25,26] Interestingly, SOA components generated from the ozonolysis of α-pinene, an isomeric monoterpene, do not form brown carbon when reacted with the same nitrogen species.[26,27] Both limonene and α-pinene are abundant volatile organic compounds, so it is important to understand their potential to modify aerosol optical properties. For example, limonene and α-pinene contribute 3–18% and 23–53%, respectively, to the total monoterpene emissions from forests in the United States.[28] Additionally, limonene is one of the five most abundant volatile organic compounds in indoor air.[29] α-Pinene and limonene are structural isomers; however, α-pinene has one fewer oxidisable double bond (Scheme 1). The differences in the aging characteristics of limonene and α-pinene ozonolysis SOA suggest that rather specific chemistry, involving second-generation products, may be important in the brown carbon formation reaction.

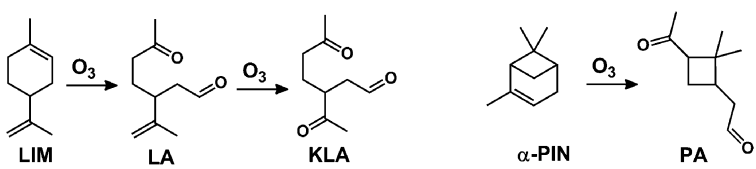

Scheme 1 Products of limonene (LIM) ozonolysis: limononaldehyde (LA) and ketolimononaldehyde (KLA), and α-pinene (α-PIN) ozonolysis: pinonaldehyde (PA).

Because the SOA mixture from the limonene/O_3 SOA does not contain significant amounts of 1,2-dicarbonyls,[30,31] its NH_4^+-mediated browning mechanism may be different from that previously-proposed for glyoxal and methylglyoxal, which produce oligomeric imidazole-based compounds in reactions with NH_4^+ and amino acids.[5–7,9,32,33] As such, the active brown-carbon precursors in the limonene/O_3 SOA mixture have yet to be identified. The study of Bones *et al.* (2010) and related studies[5,8,10,26,27,34] offer important insights on the nature of the chromophore structure and the NH_4^+-mediated reaction. These studies suggest that the chromophores likely contain a $\rangle$C=N– (imine) motif in their structures. Furthermore, it has been demonstrated that chromophores account for less than ~1% of the total aerosol mass, and have high molar extinction coefficients (possibly as high as $\sim 10^5$ M^{-1} cm^{-1}), which makes it possible for them to dominate the optical properties of the aerosol despite their low relative abundance. The NH_4^+-mediated browning of SOA proceeds through aqueous reactions under slightly acidic (pH ~ 4) to neutral conditions, and is dramatically accelerated by water evaporation from the NH_4^+ + SOA solution.[35]

Ketoaldehydes limononaldehyde (LA), ketolimononaldehyde (KLA) and pinonaldehyde (PA) are the most abundant products of ozonolysis of limonene and α-pinene. For example, PA product yields greater than 50% have been reported in ozonolysis of α-pinene,[36] while LA and KLA dominate both the gas- and particle-phase products of ozonolysis of limonene.[30,31,37] Note, this work uses the naming convention for the monoterpene oxidation products introduced by Larsen *et al.* (1998);[38] the systematic nomenclature is reported in the Electronic Supplementary Information (ESI)† section. The first-generation ketoaldehydes are semivolatile, *i.e.*, they exist mainly in the gas phase but can also be found in the aerosol phase, while the second-generation products are less volatile and are predominantly found in the aerosol phase.[30]

We hypothesized that because aldehydes are prone to nucleophilic addition (including hydration, oxidation, imine formation, *etc.*), unlike the much more stable alcohols and acids that are also present in the SOA mixture, ketoaldehydes are excellent candidates for brown carbon precursors.[39,40] To test this hypothesis, we synthesized PA, LA and KLA and aged them in the presence of NH_4^+(aq), aqueous glycine (GLY, HOOC–CH_2–NH_2), and NH_3(g) to reproduce the browning chemistry (or lack of thereof) observed in limonene/O_3 and α-pinene/O_3 SOA.

Experimental

Synthesis and purification of ketoaldehydes

LA was synthesized by the oxidative ring opening of the 1,2–epoxide of limonene, according to the procedure reported by Binder *et al.* (2008).[41] 1 mmol of limonene oxide (Aldrich, 99% purity) was continuously stirred with 2 molar equivalents of sodium metaperiodiate ($NaIO_4$, Alfa Aesar, 99.8% purity) at room temperature in 40 mL of a solvent mixture of 2 : 1 tetrahydrofuran (Aldrich, ACS grade) and water (Aldrich, HPLC grade). The reaction progress was monitored with thin layer chromatography (TLC). The concentrated crude was separated on a silica gel column (60 Å pores, 32–63 μm particles, Sorbent Tech.) with 3 : 1 hexanes/ethyl acetate mobile phase, which recovered ~80 mg of pure material after concentration under vacuum.

KLA and PA were synthesized by low-temperature ozonolysis of the corresponding pure monoterpenes using a modified procedure of Griesbaum *et al.*

(1997).[42] Specifically, 1 mmol of limonene (Acros, 97% purity) or α-pinene (Acros, 99% purity) was dissolved in ~10 mL of dichloromethane (Aldrich, ACS grade) and ozonized to completion by bubbling 1 standard litre per minute (SLM) flow of O_3/O_2 from a commercial ozone generator through the solution with continuous stirring at −78 °C. After all the double bonds had reacted, ozone started to accumulate in the solution (evidenced by a blue tint) and the flow was immediately stopped. 1.2 mole equivalent (per C=C bond) of triphenylphosphine (Alfa Aesar, 99% purity) was added and left to stir at −78 °C for 1 h, followed by stirring at room temperature for 24 h. The KLA crude was separated with a semi-prep reverse-phase liquid chromatography column (Luna C_{18}, 10 × 250 mm, 100 Å pores, 5 μm particles, Phenomenex, Inc.) coupled to a photo-diode array (PDA) UV-VIS detector (LC-UVVIS) with 2 mL min^{-1} of acetonitrile (ACN, Aldrich HPLC grade) mobile phase, affording ~35 mg of the pure material after concentration under vacuum. The PA crude was separated with semi-prep normal-phase LC-UVVIS (10 × 250 mm Luna Si, 100 Å pores, 5 μm particles, Phenomenex, Inc.) with 2 mL min^{-1} hexanes/ethyl acetate (70 : 30) mobile phase flow, affording ~70 mg of the pure material after concentration under vacuum. The appearance of the distinctive n → π* band (~280 nm) of KLA and PA in the real-time PDA spectrum was used as a prompt for the collection of carbonyl fractions, prior to purity analysis.

The purified ketoaldehyde products were characterized with ^1H nuclear magnetic resonance (NMR) spectroscopy with a 500 MHz instrument (Bruker, DRX500). The NMR spectra taken in $CDCl_3$ are shown in Fig. S1 (a–c) and the chemical shifts are reported in Table S1 of the ESI section.† The spectra are identical to those previously reported in the literature for PA,[43] LA,[44] and KLA.[42,45] Minor residual solvent impurities from ACN and HOD[46] are noted in the spectra, where applicable. Based on ^1H NMR, the purity of all synthesized compounds was conservatively estimated to be greater than 95%.

Aging experiments

The synthesized and purified ketoaldehydes were dissolved in water (18 MΩ cm, Barnstead Nanopure) with 60 °C heating and a few seconds of sonication. The aging results were negligibly affected by dissolution method. Solutions had the concentration range of 10^{-4}–10^{-3} M and were used within 2 h. Aging experiments were performed at room temperature. Small (μL) volumes of stock (20 g L^{-1}) ammonium sulphate (AS, $(NH_4)_2SO_4$) and glycine (GLY) solutions were added to 2–3 mL of the ketoaldehyde solutions at desired molar ratios ([N] : [KLA] = 0–3, where [N] refers to $[NH_4^+]$ or [GLY]), to avoid significantly diluting the ketoaldehyde solutions. We refer to AS-induced reactions as "NH_4^+-mediated" because replacing the anions in control experiments with $(NH_4)_2SO_4$, NH_4NO_3 or NH_4Cl was found to have small-to-negligible effects on the browning reactions (primarily through modification of the solution pH). The aqueous solutions of ketoaldehydes containing NH_4^+ or GLY were then evaporated to dryness using a rotary evaporator (Buchi R-210) at a bath temperature of $T = 45$ °C. The dry residue was redissolved in water to the original dilution. Unless stated otherwise, "aging" in this manuscript refers to the evaporative aging, which was demonstrated to yield the maximal chromophore formation over the course of a few minutes, as opposed to solution-phase aging or aging with NH_3 vapour, which require several days to produce the same concentration of chromophores at $\lambda = 500$ nm.[27,35] Due

to their distinctive absorption maxima, the chromophore(s) for the NH_4^+ and GLY-aged samples are referred to as "C_{500}" and "C_{520}", respectively. Control experiments without nitrogen-containing additives were performed for PA, LA and KLA and showed no detectable changes in their UV-Vis absorbance spectra.

To quantify the degree of visible light absorption, UV-Vis absorbance spectra were acquired using a dual-beam spectrometer (Shimadzu UV-2450) with purified water as the reference. The data were recorded in 1 cm quartz cuvettes in the wavelength range of 300–700 nm. Some of the samples required dilution to stay within the linearity limit of the spectrometer and data were corrected for dilution. The degree of browning is reported as the effective mass absorption coefficient (MAC, units of $cm^2\ g^{-1}$), normalized to the concentration of the organic material in SOA. MAC and ΔMAC are calculated from the base-10 absorbance A_{10} of the ketoaldehyde solution with mass concentration C_{mass} ($g\ cm^{-3}$) measured over pathlength b (cm):[47]

$$\mathrm{MAC}\ (\lambda) = \frac{A_{10}\ (\lambda)\ \times\ \ln 10}{b\ \times\ C_{\mathrm{mass}}} \quad (1)$$

$$\Delta\mathrm{MAC}\ (\lambda) = (\mathrm{MAC})_{\mathrm{aged}} - (\mathrm{MAC})_{\mathrm{control}} \quad (2)$$

MAC values ($cm^2\ g^{-1}$) correspond to the mass concentration of the starting organic material in the solution and not those of the nitrogen-containing additives that do not absorb radiation above $\lambda = 300$ nm.

Characterization of the products

Aged samples were separated isocratically with reversed-phased LC-UVVIS at 2 mL min^{-1} in (1 : 1) ACN : H_2O in order to isolate the coloured fraction. The separation was monitored in real time using a UV-VIS PDA. The C_{500} fraction containing eluted compounds that absorbed at $\lambda \sim 500$ nm was collected. The C_{500} fractions obtained from repeated injections were then combined and concentrated under vacuum. Fig. S2 in the ESI section† provides an example of one such separation. The dried residues of the separated chromophores were redissolved in solvents suitable for further analysis.

Vibrational spectra were recorded on a single-beam Fourier-transform infrared (FTIR) spectrometer (Mattson Galaxy 5000) in the spectral range of 1000–4000 cm^{-1} with a resolution of 4 cm^{-1}. For FTIR measurements, a film of the KLA was deposited onto the surface of 3 mm thick zinc-selenide (ZnSe) optical windows (Cradley Crystals Corp.). Previous experiments showed that limonene/O_3 SOA films aged with humid NH_3 vapour produced the C_{500} chromophore similar to that observed with evaporative or aqueous aging with NH_4^+.[25,27] A window with deposited KLA film was placed into a small polyethylene dish and suspended on top of a 0.5 M ammonium nitrate solution (NH_4NO_3, Fluka ACS grade) in a sealed glass container with 40 mL headspace filled with ~100 ppb of NH_3 and saturated with water vapour (predicted RH ~ 99%, measured RH ~ 85–90%).[48] The window was removed at time intervals of 0, 12, 36, and 84 h and dried under vacuum in a desiccator for several hours to eliminate condensed water prior to FTIR analyses.

Proton (^1H) and carbon (^{13}C) NMR experiments were recorded on a Bruker DRX500 (500 MHz) instrument equipped with a liquid-nitrogen cooled probe. The separated C_{500} fraction was dissolved in a (v/v) 90% H_2O (Aldrich, HPLC) /10%

D_2O (Cambridge Isotope Lab, >99.8% D) solvent mixture, and analysed with pulse-field gradient (PFG) water suppression in order to view exchangeable protons. Water-based solvent systems were used because C_{500} was found to be poorly soluble in nonpolar organic solvents (an important clue about the high polarity of the chromophores).

The separated C_{500} fraction was also dissolved in 90% H_2O/10% ACN (v/v) and analysed with high-resolution mass spectrometry (HR-MS). Data acquisition was performed with positive ion mode direct infusion electrospray ionization (ESI) using a linear-ion-trap (LTQ)-Orbitrap ($R = 100\,000$) mass spectrometer; data analyses were performed as described in our previous studies.[49,50] In direct infusion ESI/HR-MS experiments samples were injected through pulled fused silica capillary tip (50 μm i.d.) at flow rates of 0.5–2 mL min^{-1}, and the spraying voltage of 4.0 kV. All analyte compounds were observed as sodiated $(M + Na)^+$ or protonated $(M + H)^+$ species. The mass range for acquisition was m/z 100–2000 and the ESI spray voltage was 4 kV. Signals from ^{13}C were removed and molecular formulas are reported for the corresponding neutral compounds (M) by correcting for the mass of a proton or sodium atom.

We also carried out several LC-UVVIS-ESI/HRMS experiments in which the solution containing coloured products was separated on a reverse-phase column (Luna C_{18}, 5 × 150 mm, 100 Å pores, 5 μm particles, Phenomenex, Inc.), with the eluate simultaneously analysed with a photodiode array detector (Thermo Finnigan) and by HR-MS. The samples were prepared by: (a) evaporating aqueous solutions of KLA with AS, GLY, or H_2O (control), and dissolving the residue in ACN; (b) exposing a KLA film to humid NH_3 vapour for 2 days and subsequently extracting it into ACN. The absorbance of the PDA was referenced to pure methanol before each experiment. The gradient elution used a 200 μL min^{-1} flow of H_2O/ACN mixture as the eluent: 0–3 min hold at 95% H_2O, 3–43 min linear gradient to 5% H_2O, 43–53 min hold at this level, 53–56 min linear gradient back to 95% H_2O, and 56–60 min hold in anticipation of the next injection. The standard IonMAX™ ESI source was used for LC-UVVIS-ESI/HRMS experiments making it possible to send the 200 μL min^{-1} flow from the LC directly into the ion source. The settings were: 3 units of sheath gas flow, 0 units of auxiliary gas flow, 10 units of sweep gas flow, 5 kV spraying potential. The instrument was calibrated using a standard mixture of caffeine, MRFA, and Ultramark 1621 (calibration mix MSCAL 5, Sigma-Aldrich, Inc.).

Results and discussion

Ketoaldehydes as brown carbon precursors (UV-Vis)

Fig. 1 shows the quantitative wavelength-dependent ΔMAC values (eqn (2)) for NH_4^+-evaporative aging experiments at 1 : 1 molar ratios of NH_4^+ to KLA, LA and PA. Of the three ketoaldehydes, only KLA produced a significant increase in MAC upon aging. The same trends were observed for GLY-mediated aging, where KLA was once again the only ketoaldehyde that produced a coloured product mixture. Absorption spectra obtained following evaporation of a pure water solution of KLA (Fig. S3 in the ESI section†) demonstrated that KLA does not undergo browning without GLY or NH_4^+ additives. Because all three compounds (KLA, LA and PA) are 1,6-ketoaldehydes we conclude that this particular combination of functional groups is not conducive to formation of brown carbon products. KLA is

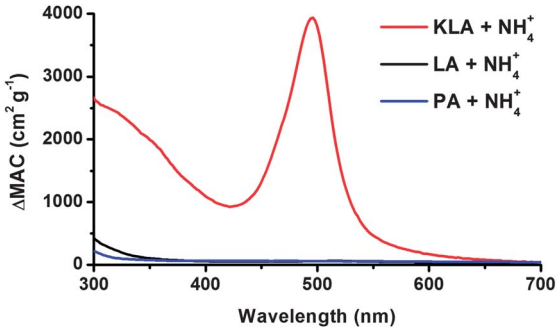

Fig. 1 Comparison of the net increase in the mass absorption coefficients ($\Delta MAC = MAC_{sample} - MAC_{control}$) between the NH_4^+-aged KLA, LA and PA.

the only compound that has an additional ketone group, providing 1,5-diketone and 1,4-ketoaldehyde moieties. The importance of these structural motifs will be illustrated in the mechanistic schemes below. Both LA and PA must be reactive towards ammonia and amino acids, but because neither LA nor PA can form brown carbon products, the remainder of the manuscript will focus on reactions of KLA.

Fig. 2 compares the absorption spectra of KLA aged by (a) NH_4^+ and (b) GLY with the spectra obtained for the aqueous extract of limonene/O_3 SOA aged in a similar manner. Compared to SOA, the shapes of the absorption spectra are almost identical. The absorption maximum for the KLA brown carbon is slightly shifted to 495 nm (compared to 500 nm in SOA), likely due to a reduction in complexity of the aged KLA mixture. Another distinctive property of brown carbon formation from limonene/O_3 SOA is the production of a 430 nm band in the initial

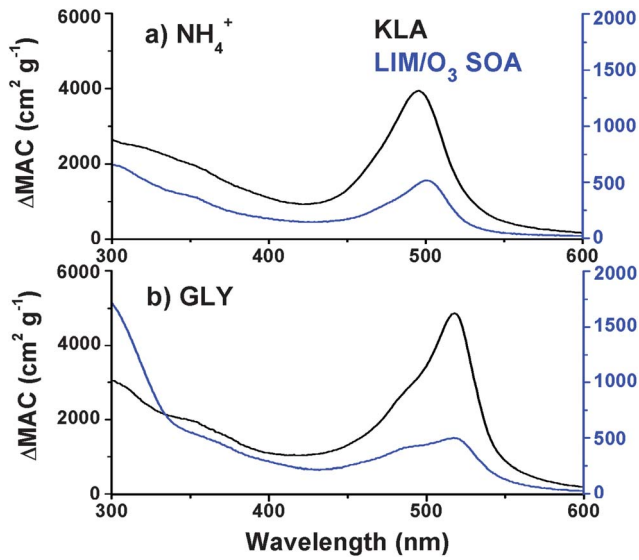

Fig. 2 Comparison of absorption spectra for brown carbon from aged KLA (black traces and left axes) and LIM/O_3 SOA (blue traces and right axes) by (a) NH_4^+ and (b) glycine.

stages of aqueous aging, which is obscured by the 500 nm band at longer timescales and upon evaporation.[26,35] Even this temporal evolution of chromophores in limonene/O_3 SOA can be reproduced by KLA (Fig. S4 in the ESI section†), offering strong evidence of similar chemistry. In the GLY-mediated aging, the absorption maxima appear at 520 nm and 518 nm for SOA and KLA, respectively. The smaller band of GLY-aged SOA at ~490 nm is also observed in the spectra of aged KLA. The observation that a single compound can reproduce the aging behaviour of the entire SOA extract suggests that the structural elements of KLA and/or its aging products are essential for brown carbon formation in the limonene/O_3 SOA organic mixture.

The aged KLA has a maximum ΔMAC value of 2000–5000 $cm^2\ g^{-1}$ at peak maximum, depending on aging method. Inherent uncertainties in the evaporation method (such as dependence of the degree of browning on the evaporation temperature)[35] lead to relatively large uncertainties in the absolute ΔMAC values. However, the relative ΔMAC values can be determined with greater accuracy by keeping the evaporation conditions identical for a series of different samples. For example, the GLY-aged KLA has systematically higher ΔMAC than NH_4^+-aged KLA. The ΔMAC values for KLA alone are higher than those for the SOA (maximum ~ 500–800 $cm^2\ g^{-1}$), which is expected because SOA contains a significantly higher fraction of non-absorbing organic mass that is included in the calculation. Based on ΔMAC ratios between the NH_4^+-aged KLA and SOA, and the assumption that KLA-like compounds are the only C_{500} precursors in limonene/O_3 SOA, we expect KLA (and its derivatives) to be initially present in the SOA at roughly 10–40% mass. Although a KLA yield in limonene ozonolysis has not been reported, this value is qualitatively in agreement with the expectation that KLA is the most abundant single component of limonene/O_3 SOA.[30]

Effective stoichiometry of reaction (UV-Vis)

We investigated the dependence of the evaporative KLA + NH_4^+ and KLA + GLY reactions on the molar concentration of KLA and added nitrogen compounds. Fig. 3 shows that for a fixed initial concentration of KLA, an increase in the

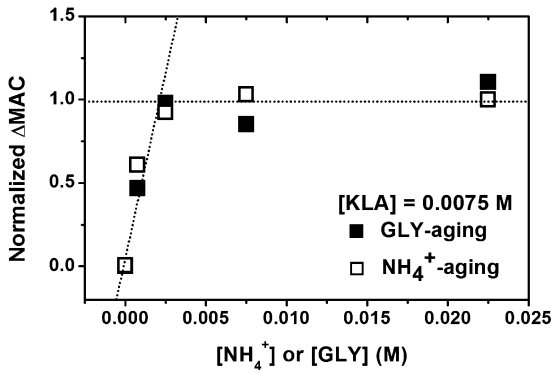

Fig. 3 Dependence of chromophore formation on the molar concentration of reduced nitrogen compound added. The MAC values for NH_4^+ and GLY aging are normalized by the maximum to be on the same scale for clarity. The effective reaction stoichiometry of [N]/[KLA] ~ 1/3 can be determined from the location of the break in the concentration dependence.

amount of added nitrogen compounds enhances ΔMAC until a plateau is reached. We previously showed that the absorbance by the chromophores obeys Beer's law,[27] therefore, the ΔMAC values of chromophoric species should be directly proportional to the overall concentration of chromophoric products. If we assume that reaction $a(NH_4^+$ or GLY) + bKLA → P goes to completion upon evaporation (P = chromophoric products), the effective stoichiometric ratio a/b can be determined from the concentration of $[N]_{plateau}$ (N = GLY or NH_4^+) at which the break in the dependence occurs. For both NH_4^+ and GLY the plateau is reached at ~2.5 mM when the initial KLA concentration is 7.5 mM indicating the reaction stoichiometric ratio is $(a/b) = [N]_{plateau}/[KLA]_0 \sim 1/3$. Experiments in which the initial [N] was fixed and [KLA] varied led to a similar conclusion: the relative initial slopes in the MAC *vs.* [KLA] and MAC *vs.* [N] plots also gave $a/b \sim 1/3$. The reactions of KLA with NH_4^+ and GLY have similar concentration dependence, presumably because NH_4^+ and amines initially react with aldehydes by the same mechanism. With the assumption that reduced nitrogen reacts with only the aldehyde group, a 1/1 stoichiometry would be expected for the reaction. The observed stoichiometry of N/KLA ~ 1/3 indicates that the reactions leading to the chromophores (P = C_{500} or C_{520}) may involve as many as three KLA units. As we discuss below, a number of compounds observed in HR-MS experiments with KLA + NH_4^+ have chemical formulas of $C_{27}H_xNO_y$, which can be formed by combining one ammonia molecule and three molecules of KLA ($C_9H_{14}O_3$). However, a number of other products with different N/KLA combinations are also observed, therefore, the empirically determined 1/3 stoichiometry should be regarded as an average over a large number of light-absorbing products.

Importance of the aldehyde to imines conversion in browning (FTIR and NMR)

Because the absorption spectra and reaction of the NH_4^+- and GLY-mediated chromophores are qualitatively similar, and because of the larger environmental relevance of NH_4^+, we focused on structure analysis of only the NH_4^+-based chromophore (C_{500}). Direct application of FTIR to the evaporated residues or redissolved KLA + NH_4^+ mixtures was complicated by interference from solvent and inorganic additives. As an alternative, we investigated aging of a pure KLA film with humid NH_3 vapour that was monitored with FTIR at four time intervals (Fig. 4). Although aging of a film with humid NH_3 vapour produces similar chromophores to those formed in evaporative aging,[25] it is much slower and may be limited by the surface area of the film. However, this method of aging eliminates interference from the inorganic additives, for example, the interfering bands such as the strong NH bending modes of NH_4^+ (expected at ~1400 cm^{-1})[51] are absent in the spectra.

Based on the expected chemistry,[25,27] the characteristic bands associated with the vibrations of the reactive carbonyl groups in KLA should be augmented or replaced by the new bands corresponding to C–N (amines) and C=N (imines) and other aging products. The pure KLA (Fig. 4, black trace) film is characterized by aliphatic CH_3/CH_2 stretches (2800–3000 cm^{-1}) and bends (1300–1500 cm^{-1}) that are relatively broad, suggesting a disordered film. A broad peak at ~3430 cm^{-1} indicate a hydrogen-bonded OH stretching band, presumably of an intramolecular aldol of KLA, diol (hydrated KLA), or carboxylic acid (oxidized KLA). The relatively small width and symmetric shape of the C=O stretch at 1710 cm^{-1}

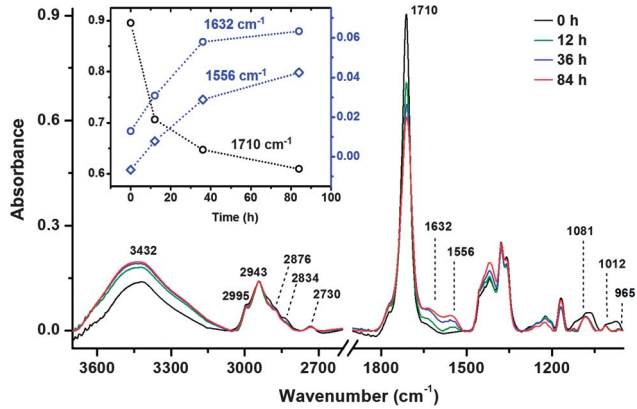

Fig. 4 Infrared spectra of the KLA film aged with humid NH_3 vapours at four aging times. Inset shows time profiles of select bands (see text).

rules out high acid contribution to the film at the early stages of reaction (^{1}H NMR spectra indicate that the pure KLA does not have COOH contamination). The broad peak around 3430 cm^{-1} overlaps the hydrogen-bonded N–H stretches, of pyrroles for example,[52,53] or of absorbed water, which limits its analytic usefulness. The aldehyde functionality is confirmed by two weak bands unique to aldehydes: the C(O)–H stretch at 2834 cm^{-1} and the first overtone of the in-plane C(O)–H bend at 2730 cm^{-1}, which gains intensity because of the Fermi resonance with the stretch.[54,55] The two C(O)–H bands and the carbonyl C═O band at 1710 cm^{-1} are reduced in intensity relative to the skeletal C–H vibrations as the reaction progresses confirming that the carbonyls groups in KLA react with NH_3 and water vapour. After 84 h of exposure of the KLA film to the humid NH_3 vapour, the reaction is not complete, *i.e.*, most of the original vibrational bands of KLA are still present. Because the dried KLA is viscous, substantial diffusion limitation likely exists in the film; therefore, the reaction may be limited to the surface and eventually ceases, even when unreacted KLA is still present.

As the film experiences aging by NH_3(g), several new bands appear at 1012, 1082, 1070, 1556 and 1632 cm^{-1}. In addition, the bands between 1300 and 1500 cm^{-1} slightly increase in intensity. The new peaks with the highest diagnostic potential are those at 1632 and 1556 cm^{-1}, which are consistent with the presence of nitrogen-containing bonds in the products. The growth of these peaks and the decay of the carbonyl peak are shown in the insert in Fig. 4. The alternative assignment of the 1632 cm^{-1} band to a conjugated C═C stretch, that would also appear in the 1610–1640 cm^{-1} spectral region, can be ruled out because of the lack of the corresponding vinyl CH stretches in the spectrum (>3000 cm^{-1}, frequency increasing with the level of conjugation). In particular, the 1556 cm^{-1} band may correspond to an N–H bending mode and the 1632 cm^{-1} band may correspond to the C═N stretching mode of substituted imines (or Schiff bases)[56,57] or N-heterocycles like pyrroles.[58] Bones *et al.* (2010) also suggested that a protonated Schiff bases may play a role in the visible light absorption,[26] as they can be highly absorbing when only moderately conjugated.[59] Given the nature of reaction, the presence of pyrroles may be equally likely (discussed in more detail

below). Amides, which have so called amide-I and amide-II bands in this frequency range,[55] are not expected to form from carboxylic acids under the aging conditions employed in our experiments (and there is no evidence for them in the NMR experiments described next).

The C_{500} fraction was analysed by NMR spectroscopy to supplement FTIR observations. We note that NMR does not necessarily probe the same compounds as FTIR because: (a) NMR was performed on the C_{500} fraction of the KLA + NH_4^+ evaporated sample, whereas FTIR was performed on the entire KLA + NH_3(g) mixture with a large signal contribution from the intact KLA in the film throughout the reaction and (b) the NMR samples are dissolved in $CDCl_3$ or H_2O/D_2O and the FTIR samples have no solvent apart from the residual absorbed water. Furthermore, the same molecules may exist in different chemical forms, such as open, aldol, hydrated, *etc.*, depending on the type of the sample, presence or absence of water, and measurement method. We have taken these factors in consideration in our data analysis.

Fig. 5a shows the KLA ^{1}H NMR spectrum in $CDCl_3$, which can be compared with the ^{1}H spectrum of C_{500} fraction taken in H_2O, with water suppression, shown in Fig. 5b. Based on the shape of the peaks in the alkyl region, C_{500} fraction contains one major component and several minor ones. The major C_{500} products

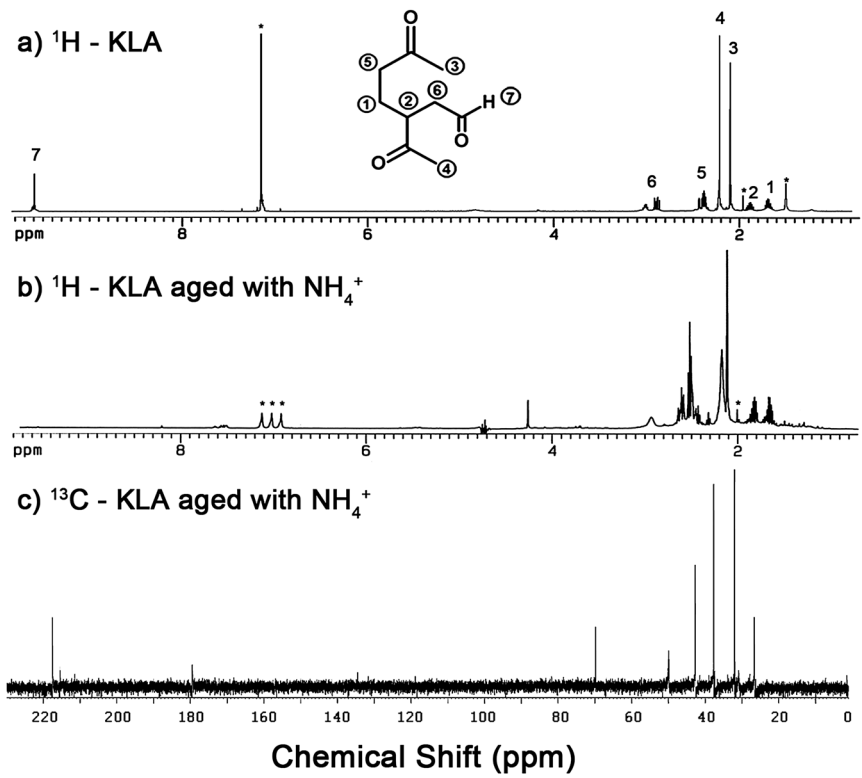

Fig. 5 Proton (^{1}H) NMR spectra of (a) KLA taken in $CDCl_3$ and (b) the separated coloured fraction of KLA aged with NH_4^+ taken in H_2O/D_2O (9 : 1) with PFG water suppression. The carbon (^{13}C) spectrum of the aged/separated KLA fraction taken in H_2O/D_2O (9 : 1) is shown in panel (c). Residual solvent or inorganic resonances are shown with asterisks, from right to left: (a) HOD, ACN, $CDCl_3$; (b) ACN, NH_4^+; (c) none.

retained several resonances characteristic to KLA including the ketone CH_3 proton groups (although one of them is broadened) and protons from the main carbon skeleton such as those labelled "1" and "2" in Fig. 5a. The aldehyde proton at 9.7 ppm (labelled "7" in Fig. 5a and Fig. S1† for pure KLA) is no longer present, in good agreement with the reduction of the C(O)–H vibrations observed in FTIR. Aldehydes are known to hydrate in water but if hydration was the only mechanism operating in the solution, we would still observe the aldehyde proton based on the expected hydration equilibrium ratio for aldehydes of this size. The removal of the aldehyde group most likely results from an intramolecular aldol formation *via* a ketone enol adding to the aldehyde group, which can be catalysed by NH_4^+,[60] or from the nucleophilic addition of reduced nitrogen compounds. These types of reactions are slow in solution but are promoted by evaporation because water is a product. Several different enols and intramolecular aldols can be formed from KLA, but based on product yields from similar 1,6-ketoaldehydes, *e.g.*, 6-oxo-heptanal,[61] the aldol with a 5-member ring should be preferentially formed from nucleophilic attack at the aldehyde site.

Several unique major and minor resonances for C_{500} are observed in the alkyl (1–3 ppm) region, which cannot be assigned conclusively. The singlet at 4.3 ppm is most consistent with an alcohol proton. This singlet does not show up in the C_{500} spectrum taken in D_2O (Fig. S5 in the ESI section†) because alcohol protons are exchangeable with the solvent (OH → OD) and become silent. The observation of the alcohol proton is also consistent with a cyclic aldol as a major product. The trio of peaks at around 7 ppm belongs to the NH protons of the ammonium ion.[33] Although the C_{500} fraction has been separated, NH_4^+ may be present in the sample due to complexation with water-soluble organics or decomposition of nitrogen-containing compounds. These NH protons also exchange with the solvent and consequently are also absent in the D_2O spectrum (Fig. S5†).

The ^{13}C proton-decoupled spectrum of C_{500} taken in H_2O, shown in Fig. 5c, is more straightforward to interpret. Each resonance belongs to a carbon atom in a unique electronic environment and unlike ^1H NMR, ketones may be straightforwardly identified. The first useful observation is that the number of the observed peaks is relatively small, of the order of 10. This implies that the major C_{500} fraction's component is a molecule that is comparable in size to KLA which has 9 chemically distinguishable carbon atoms. The 25–45 ppm region corresponds to various types of alkyl carbons and transitions from 1°–3° aliphatic carbons in the direction of higher chemical shift. The 27 ppm peak can be assigned to a cyclic CH_2 group. The most downfield shifts at 218 ppm correspond to cyclic ketones (less shielded than an aliphatic ketone). Another small peak at 216 ppm may also be assigned to a ketone from a minor species. Similarly to the ^1H spectrum, no aldehyde carbons, ~200 ppm, can be observed. The resonance at 70 ppm is most likely due to carbon atom attached to hydroxyl functional group. The 50 ppm resonance may be assigned to a 1°–2° carbon atom attached to nitrogen by a single bond (C–NH), although in some cases 2°–3° alkyl carbons can show up in this region.

The ^{13}C NMR data are consistent with the suggestion by ^1H NMR that a cyclic aldol with a ketone functional group (but no aldehydes) is the primary component in the aqueous solution of the C_{500} fraction, which co-exists in solution with a few minor organics that may or may not contain nitrogen. The dominant structures implicated by NMR are not the species that absorb visible light because all

possible monomeric KLA aldols are expected to be colourless. Although we used LC-UVVIS to specifically isolate the light-absorbing compounds, the aldol compound(s) could coincidentally co-elute with them or be produced from them by hydrolysis of C_{500} in water.

Based on this and previous works,[35] the chromophore is likely a *minor species* whose signals are smaller, and possibly below the detection limit, compared to the more-dominant FTIR and NMR signals. Very weak ^{13}C resonances in the 120–140 ppm region of the ^{13}C spectrum provide useful indications that conjugated and/or aromatic carbons (–C═C–) exist in the C_{500} mixture. Another weak resonance at approximately 180 ppm may be assigned to either a COOH or C═N carbon; however, C═N is more consistent with the FTIR observations. We suspect these weak resonances are most indicative of the brown carbon chromophores, because it may take substantial conjugation and nitrogen substitution to promote light absorbance in the visible region. The fact that no obvious vinyl CH stretches (>3000 cm^{-1}) were discernible in the aged FTIR spectra is also consistent with small relative fraction of the chromophore amongst the products of aging. In summary, these observations suggest that the major functional groups in the C_{500} fraction compounds are hydroxyls and carbonyls, with minor contributions from amines, imines (or N-heterocycles that cannot be distinguished from secondary imines by NMR), and carboxyls.

Charged nature of the coloured compounds (HR-MS)

In order to provide molecular level information about the chromophores, the C_{500} fraction was analysed by direct infusion high-resolution ESI-MS. The coloured residues formed in the evaporation of KLA + NH_4^+ and KLA + GLY mixtures, as well as the products formed by browning of a KLA film with humid NH_3 vapour, were additionally analysed with LC-UVVIS-ESI/HRMS. The analysis was also performed for the products of reactions of limonene/O_3 SOA and NH_4^+ for comparison. Representative chromatograms corresponding to the integrated 400–600 nm absorbance are shown in Fig. 6. The SOA + NH_4^+ (Fig. 6a) and KLA + NH_4^+(Fig. 6b) chromatograms are qualitatively similar but the former contains far more peaks than the latter. In fact, the NH_4^+-aged KLA chromatogram has only two distinct features: two overlapping sharp peaks eluting at 2–3 min and a single broad peak eluting at 13–36 min. The early-eluting fraction corresponds to the C_{500} fraction isolated on the LC separation stage and discussed extensively in the previous sections. The 500 nm absorption band is distinctively observed in the absorption spectra for both early- and late-eluting coloured fractions (Fig. S6 in the ESI section†). GLY-aged and NH_3-aged KLA resulted in qualitatively similar chromatograms (not shown in Fig. 6).

The early peaks in the chromatograms elute close to the column's dead time together with the charged inorganic mixture constituents, such as HSO_4^-. We therefore suspect that a significant fraction of compounds eluting early either carry a permanent charge or are zwitterions. Indeed, the observed molecular formulas of the compounds eluting early (Table 1) correspond to fairly large organic molecules (mostly C_9–C_{27}), which would be expected to elute considerably later than at 2–3 min if they remained neutral during their passage through the column. This is consistent with our observation that the LC-separated C_{500} fraction, which also eluted close to the column's dead time (Fig. S2 in the ESI

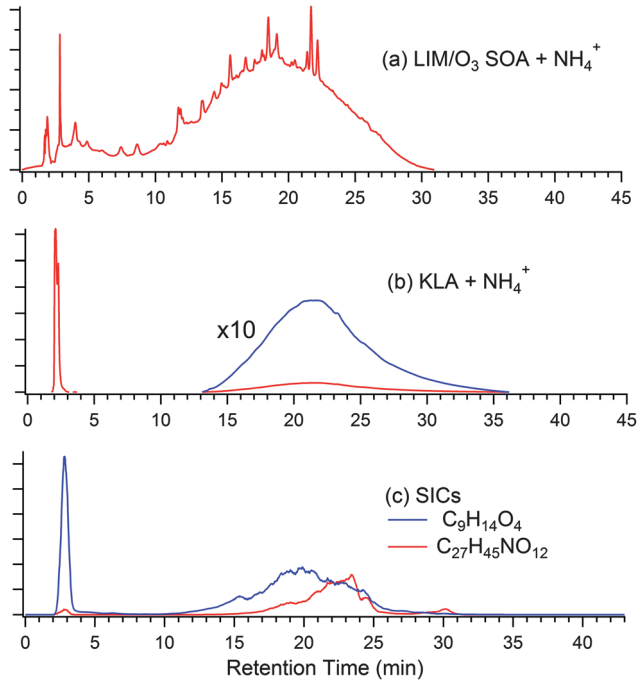

Fig. 6 Sample LC-UVVIS-ESI/HRMS (integrated 400–600 nm absorbance) chromatograms of the NH_4^+-aged (a) aqueous SOA mixture and (b) aqueous KLA extract. The blue trace in panel (b) corresponds to a tenfold magnification of the late-eluting signal. Panel (c) shows selected ion chromatograms (SICs) for protonated $C_9H_{14}O_4$ and $C_{27}H_{45}NO_{12}$. SICs for most other ions displayed a similarly poor level of chromatographic resolution.

section†), was not soluble in non-polar solvents but dissolved readily in water and ACN. It is likely that KLA-derived brown carbon contains ionic or zwitterionic compounds for which the reversed-phase chromatography used in this work is not sufficient.

The lack of resolution in the late eluting broad peak for the KLA + NH_4^+, KLA + GLY, and KLA + NH_3 samples was a surprise. We note the separation column works quite well for many mixture components in the SOA + NH_4^+ sample, as evidenced by multiple well resolved peaks appearing throughout the chromatogram (Fig. 6a). One possible explanation for the lack of resolution is a very large number of products with comparable elution times. However, this assumption is not consistent with selected ion chromatograms (SICs), which display a similarly low level of chromatographic resolution. For example, Fig. 6c shows a SIC for protonated $C_{27}H_{45}NO_{12}$, which elutes as a broad peak between 15 and 30 min. This behaviour is characteristic of most other ions we have examined. Therefore, the peak broadening must arise from a chemical reason, perhaps from keto–enol tautomerization, multiprotic acid–base, and hydration–dehydration equilibria occurring during the separation.

The most abundant molecular formulas reproducibly observed in the LC-ESI/HRMS and the direct infusion ESI/HRMS are listed in Table 1. Most of the observed compounds have carbon skeletons traceable to KLA, *e.g.*, monomers (C_9), dimers (C_{18}), trimers (C_{27}), and tetramers (C_{36}). However, in source

Table 1 The most abundant neutral molecular formulas observed in the positive ion mode direct infusion ESI/HRMS measurements on the C_{500} fraction in mixed water/ACN (50 : 50 v) solvent and in the LC-UVVIS-ESI/HRMS measurements on the KLA + NH_3(g) sample in H_2O/ACN eluent at mixing ratios of 95 : 5 v (2–3 min elution time) and 75 : 25–39 : 61 v (14–30 min elution time). We note that differences in mixing ratios of solvent as well as difference in ionization sources may be responsible for the distribution of the MS peak intensities of the observed species. The charge carrier in the LC-ESI/HRMS measurements was H^+ in most cases. The last three columns contain relative intensities, scaled to 100%, for the compounds eluting between 14–30 min and 2–3 min in the LC-ESI/HRMS experiments, and compounds detected by direct infusion ESI-MS, respectively

# C	# H	# O	# N	DBE	LC-ESI/HRMS eluted at 14–30 min	LC-ESI/HRMS eluted at 2–3 min	ESI/HRMS direct infusion
7	8	1	0	4	9.1	1.6	
7	8	2	0	4	8.9	2.7	
7	10	2	0	3	57.0	5.5	
7	10	3	0	3	23.2	1.6	
8	10	1	0	4	5.8	2.4	
8	10	2	0	4	4.2	1.1	
8	10	3	0	4	1.7	3.2	
8	12	2	0	3	13.2	2.3	
9	10	2	0	5	51.8	51.8	14.5
9	10	3	0	5	4.5	4.1	
9	11	2	1	5		0.4	1.7
9	12	2	0	4	100.0	100.0	2.7
9	12	3	0	4	71.0	49.9	18.5
9	12	4	0	4	5.8	3.1	1.3
9	13	1	1	4		0.9	1.3
9	13	2	1	4			1.1
9	14	3	0	3	4.0	2.8	4.7
9	14	4	0	3	26.4	11.0	100.0
9	14	5	0	3	0.8	0.9	7.6
9	16	5	0	2			1.4
9	17	4	1	2			2.4
10	13	1	1	5	2.1	54.7	
10	13	2	1	5	0.3	11.0	
11	15	1	1	5		10.6	
11	15	2	1	5	0.6	19.3	
11	16	1	2	5		4.9	
18	20	3	0	9	0.3		
18	23	3	1	8	0.3	3.8	0.1
18	24	6	0	7	3.4		
18	26	7	0	6	9.3	1.2	
18	26	8	0	6	5.3	0.4	
18	28	8	0	5	2.0		0.6
18	28	9	0	5	1.0		0.7
18	31	8	1	4	25.8		
18	31	9	1	4	17.2	1.4	
18	33	10	1	3	17.0	1.0	
18	33	11	1	3	4.4	0.5	
20	24	2	2	10	0.4	10.7	
20	24	3	2	10	0.4	7.6	
20	26	4	2	9	0.2	2.8	3.1
21	24	2	2	11		4.1	
21	26	2	2	10	0.9	28.9	
21	26	3	2	10	0.6	21.9	
21	27	2	3	10	0.2	7.5	

Table 1 (*Contd.*)

# C	# H	# O	# N	DBE	LC-ESI/HRMS eluted at 14–30 min	LC-ESI/HRMS eluted at 2–3 min	ESI/HRMS direct infusion
21	29	2	3	9		4.0	
27	43	10	1	7	6.3		
27	43	11	1	7	3.5		
27	45	11	1	6	5.2		
27	45	12	1	6	14.4		
27	45	13	1	6	16.6	0.5	
27	45	14	1	6	6.0		
27	47	13	1	5	4.9	0.4	
27	47	14	1	5	5.8	0.6	
36	59	16	1	8	3.3		
36	59	17	1	8	3.4		

fragmentation, multistep chemistry (*e.g.*, oligomerization combined with decomposition reactions like decarboxylation), or direct contamination introduced by the synthesis and evaporation may be responsible for the appearance of molecular formulas with carbon numbers that are not multiples of 9, such as C_7, C_8, C_{10}, C_{11}, *etc.* Several dominant species that appear at essentially all retention times, such as protonated $C_9H_{12}O_2$, likely correspond to common fragments of larger compounds. For example, the protonated $C_9H_{14}O_4$, a compound that cannot be a chromophore itself in view of its small size and DBE, co-elutes with both early-eluting and late-eluting absorbers (Fig. 6c). It is also the most dominant compound detected in the direct infusion ESI/HRMS experiments.

The majority of the observed products contain 0–2 N-atoms in their molecular formulas and double bond equivalencies (DBE = the total number of double bonds and rings) in the range of 3–10. A significant fraction of the observed compounds appear to be "built" from three KLA molecules (C_{27} skeleton) and one N-atom, in agreement with the 3 : 1 stoichiometry suggested by the optical absorption measurements (Fig. 3). However, a number of 1 : 1, 2 : 1, and other KLA : N combinations are also observed. Fig. S7 in the ESI section† provides a pictorial representation of the observed compounds as a graph of the (O + N)/C ratio *vs.* the number of C-atoms in the molecules. Reactions that form imines from carbonyls are expected to conserve the (O + N)/C ratio, while the condensation reaction leading to oligomerization and loss of water are expected to lower it relative to the starting (O + N)/C ratio of 0.33 in KLA. While most compounds do follow this trend a number of other compounds have (O + N)/C ratios in excess of 0.33, implying that some products are oxidized (increased O) and/or are present as the β-hydroxy secondary amines (*e.g.*, from hemiaminal addition to the aldehyde prior to dehydration, see Scheme 1 or Scheme S1†). Indeed the major ion detected by ESI-MS is $C_9H_{14}O_4$ = KLA oxidized to ketolimononic acid (existing in its intramolecular aldol form according to the NMR observations).

Some compounds with high DBE (= 10–11), and 2 nitrogen atoms cannot be traced directly to the KLA structure. One may speculate that the higher nitrogen content, higher DBE and unusual carbon number of compounds like $C_{21}H_{24}N_2O_2$ (DBE = 11) are due to reactions favouring the elimination of carbon to yield an aromatic product. For example, the hetero retro Diels–Alder reactions of cyclic

imines,[62–64] a reaction that may occur at room temperature and is enhanced by protic solvents. The result may be the oligomeric N-heterocyclic compounds that are suggested to play a role in the light-absorbing properties of other types of secondary brown carbon.[10,33,34,65] However, due to the uncertainty in their formation pathways starting from KLA, a representative structure for these 2N compounds cannot be determined based on the results of this study.

Possible production pathways of light-absorbing species

Most of the compounds observed by NMR and HR-MS are not expected to absorb visible radiation due to their low DBE and small molecular size. The proposed formation pathways of monomers and oligomers corresponding to many of the molecular formulas detected in HR-MS, based on a few well-known reactions, are shown in Scheme S1 of the ESI section.† Full discussion of compounds that don't absorb visible light is outside the scope of this work. We focus our attention on the molecular formulas with high DBE, which may correspond to chromophoric compounds. Although these molecules produce a much lower signal in HR-MS relative to the most abundant ions, they are likely to dominate the visible absorbance by the mixture. This makes their identification comparable to finding a "needle in a haystack".

Another complication is that multiple isomeric structures may correspond to a given molecular formula inferred from HR-MS. However, we can narrow down the spectrum of probable candidates based on the available analytical evidence (from UV-VIS, FTIR, NMR, and LC) and provide examples of reactions that may generate plausible structures. Our observations support the following picture: (1) fast disappearance of the aldehyde group to form aldols and compounds with >C=N– groups (imines or N-heterocycles); (2) a relatively large product pool with an abundance of simple monomers that don't absorb visible light and a smaller mass fraction of brown carbon chromophores; and (3) compounds containing 0–2 N-atoms found in the mixture with high degrees of unsaturation that may contribute to the light-absorption properties of C_{500}. Scheme 2 shows examples of the proposed formation routes to three 0N, 1N and 2N compounds that have the

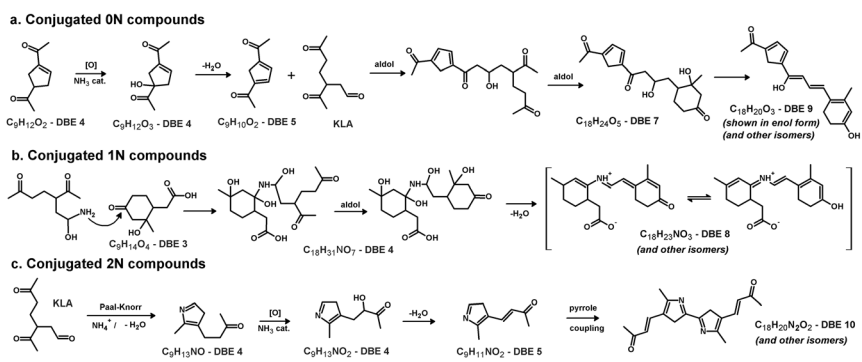

Scheme 2 Proposed formation of plausible highly-conjugated species in C_{500} that may contribute to the visible-light-absorbing properties of C_{500}. Likely, many isomers and higher-order oligomers exist. Molecular formulas shown in the scheme, with their proposed corresponding structures, have been detected with HR-MS (Table 1).

highest DBE in the mixture (Table 1). We are not suggesting that these are the actual structures of the chromophores and the precise mechanism leading to their formation – most likely, a number of alternate pathways exist that lead to similar compounds or their structural isomers. Furthermore, although the products shown in Scheme 2 have the highest DBE observed in this work, it does not imply that those explicit compounds contain enough conjugation and the correct functional group distribution to absorb visible light. Electronic structure calculations would be useful in answering this question in the future.

Scheme 2a shows the formation of a conjugated compound with molecular formula $C_{18}H_{20}O_3$ (DBE = 9), starting with the dominant aldol condensate from KLA. The ketone group can undergo NH_3- or amino acid-catalysed α-hydroxylation,[66] or in the case of α,β-unsaturated ketones, γ-hydroxylation,[67] both yielding a cyclic diene diketone with molecular formula $C_9H_{12}O_2$ (DBE = 5) that is detected in C_{500} with significant signal (Table 1). In the α-hydroxylation of a ketone in the presence of ammonia, the ketone is first transformed into an enolate or enamine, and subsequent oxidation of the C=C bond in water affords the α-hydroxylated product that can dehydrate further to form a conjugated product. The diketone may react with KLA by intermolecular enol addition to the KLA aldehyde. Subsequent aldol condensations affords $C_{18}H_{20}O_3$ (DBE = 9), a compound that is highly-conjugated if most of its ketones are present as enols, expected to be the dominant form in situations where a large π- system results from the tautomerization.[61] The proposed structure is not expected to be permanently charged, in good agreement with its absence in the early-eluting chromatographic peak. Its ability to tautomerize may lead to its detection as part of the broad peak at later retention times (Table 1). The product of Scheme 2a has 7 linearly-conjugated double bonds. Comparatively, the highly-coloured carotenoids (a large class of mainly $C_xH_yO_z$ chromophores) that absorb around 500 nm have 10–13 conjugated double bonds. It is possible that a conjugated KLA trimer can be formed in a similar manner as shown in Scheme 2a, which would further extend the π-system for 0N chromophores, but its signal lies below the detection limit of our instrument.

Scheme 2b shows the formation of a conjugated compound with molecular formula $C_{18}H_{23}NO_3$ (DBE = 8), one of the observed products of KLA aging (Table 1). This compound was also one of the major N-containing species detected by the DESI/HR-MS analysis of limonene SOA exposed to NH_3 vapour.[25] The proposed scheme starts with the formation of a hemiaminal intermediate of KLA that can nucleophilically add to a carbonyl,[68] such as the aldol acid version of $C_9H_{14}O_4$. The product is a α-hydroxy secondary amine, with subsequent dehydration yielding a Schiff base ($R_1R_2C = NR_3$, $R_3 \neq H$). The end product in Scheme 2b has 5 linearly-conjugated double bonds. Because the proposed $C_{18}H_{23}NO_3$ Schiff base is an organic compound containing both an imine group and a carboxylic acid group, strong intramolecular H-bonding (*via* a 7-member ring) may lead to zwitterion formation by protonation of the imine by the acid.[69] We note there are other reaction pathways leading to a $C_{18}H_{23}NO_3$ molecule stemming from the observed compounds in aqueous media, such as organic acid-catalysed Mannich-type reaction between enols and imines[70,71] or transimination of an imine and amine.[72–74] However, the proposed reaction mechanism satisfies the following criteria: it requires only mild organic acid catalysis and it occurs in aqueous solution. Because absorbance of Schiff bases can shift significantly to the

red due to protonation at the nitrogen site, the protonation of the imine is expected to greatly enhance the visible light absorption of this molecule. For example, the non-protonated form of the 11-*cis*-retinal + *n*-butylamine Schiff base (6 conjugated double bonds) absorbs at ~350 nm in methanol, but its protonated form absorbs at ~450 nm.[75,76] The suggestion of a protonated Schiff base is supported by these molecules' short retention time in a C_{18} column and the similarity in the shape of absorbance spectra and high extinction coefficients ($>10^4$ M^{-1} cm^{-1}) of C_{500} with that of the *cis*-11 retinal Schiff base.[59] Therefore, even though the product of Scheme 2b contains less conjugation than the product of Scheme 2a, the presence of a zwitterionic secondary imine makes it more likely to contribute to the visible light absorption.

Scheme 2c shows the formation of a conjugated compound with molecular formula $C_{18}H_{20}N_2O_2$ (DBE = 10), starting with the Paal–Knorr pyrrole formation from the 1,4-dicarbonyl moiety of KLA with either NH_4^+ or amino acid.[77,78] Presumably, a hemiaminal is formed at the keto site from the nitrogen addition, which adds to aldehyde and subsequent dehydration forms the pyrrole. Pyrroles couple easily, especially in water at neutral pH.[79] Dimerization produces a 2N compound joined at the α-carbon. Multiple stages of the reaction may occur for the pyrrole compound, producing higher-order oligomers; however, pyrroles from KLA do not have a second unsubstituted α-carbon site to produce polymers. Furthermore, pyrrole polymers, although highly-absorbing, are also insoluble or poorly-soluble in polar solvents,[80] in stark contrast to C_{500} where the brown colour disappears upon dissolution of the aged KLA in nonpolar solvents. Pyrroles may stabilize a positive charge reasonably well due to their basic N, which may be the reason $C_{18}H_{20}N_2O_2$ elutes only at the early retention time. The product of Scheme 2c has 8 linearly-conjugated double bonds; however, similar structures have not been studied in the literature so a direct comparison of optical characteristics is not possible at this time. It's worth noting that the polypyrroles that are insoluble in water have absorption spectra remarkably similar to C_{500}, and the degree of conjugation can be very high.[81,82] Bipyrrole ($C_8H_8N_2$) itself does not absorb at wavelengths greater than 300 nm;[83] however, it is not clear how additional π-conjugation will change its absorption characteristics.

Conclusions and implications

The reaction of KLA was demonstrated to form brown carbon chromophores that are nearly identical in properties to those found in the limonene/O_3 SOA upon aging with NH_4^+ and GLY. In contrast, comparable NH_4^+- and GLY-mediated reactions with LA or PA did not result in brown carbon formation. The analytical insights obtained from spectrometric methods suggest the contribution of conjugated compounds, *e.g.*, aldol condensates, secondary imines (Schiff bases), or N-heterocycles like pyrroles, to the optical properties of the chromophores. They form by different mechanisms than the imidazole-based oligomers previously linked to secondary brown carbon in the atmospheric chemistry literature.[7–10,33,34] As the chemistry that produces brown carbon is diverse, the structures of the chromophoric compounds may be similarly varied in nature.

This work emphasizes the importance of molecular structure in chemistry affecting important physical properties of aerosols, namely their optical absorption coefficient. It would not be possible to predict the occurrence of the reactions

described in this manuscript from average properties of aerosols alone, such as the O/C ratio, which is frequently used in correlating physical properties to the average composition. Even information about presence or absence of specific functional groups in the aerosol may not be sufficient. For example, KLA, LA, and PA are all ketoaldehydes but only one of them browns in reactions with ammonium ions. Therefore, it is not enough to characterize the average aerosol composition and the functional group content – the detailed molecular structures of aerosol constituents must be characterized in order to predict its aging chemistry and optical properties.

Acknowledgements

The authors would also like to thank the following people for helpful discussions: Dr John DeLorbe, Dr Phil Dennison, Dr Hyun Ji (Julie) Lee, Dr Jiri Misek, Dr Theresa McIntire, Dr John Greaves, Prof. Richard Chamberlain, and Prof. James Nowick. The UCI group acknowledges support by the NSF grants CHE-0909227 and AGS-1227579. TBN thanks UCI for the Chancellors Club fellowship. The PNNL group acknowledges support from the Chemical Sciences Division (JL), Office of Basic Energy Sciences of the U.S. DOE, and the W.R. Wiley Environmental Molecular Sciences Laboratory (EMSL) – a national scientific user facility located at PNNL, and sponsored by the Office of Biological and Environmental Research of the U.S. PNNL is operated for US DOE by Battelle Memorial Institute under Contract No. DE-AC06-76RL0 1830.

References

1 S. Solomon, D. Qin, M. Manning, Z. Chen, M. Marquis, K. B. Averyt, M. Tignor and H. L. Miller, *Climate Change 2007: The Physical Science Basis. Contribution of Working Group I to the Fourth Assessment Report of the Intergovernmental Panel on Climate Change.*, IPCC, 2007.
2 M. O. Andreae and A. Gelencser, *Atmos. Chem. Phys.*, 2006, **6**, 3131–3148.
3 T. Bond and R. Bergstrom, *Aerosol Sci. Technol.*, 2006, **40**, 27–67.
4 D. T. L. Alexander, P. A. Crozier and J. R. Anderson, *Science*, 2008, **321**, 833–836.
5 M. M. Galloway, P. S. Chhabra, A. W. H. Chan, J. D. Surratt, R. C. Flagan, J. H. Seinfeld and F. N. Keutsch, *Atmos. Chem. Phys.*, 2009, **9**, 3331–3345.
6 B. Noziere, P. Dziedzic and A. Cordova, *J. Phys. Chem. A*, 2009, **113**, 231–237.
7 E. L. Shapiro, J. Szprengiel, N. Sareen, C. N. Jen, M. R. Giordano and V. F. McNeill, *Atmos. Chem. Phys.*, 2009, **9**, 2289–2300.
8 N. Sareen, A. N. Schwier, E. L. Shapiro, D. Mitroo and V. F. McNeill, *Atmos. Chem. Phys.*, 2010, **10**, 997–1016.
9 M. Trainic, A. Abo Riziq, A. Lavi, J. M. Flores and Y. Rudich, *Atmos. Chem. Phys.*, 2011, **11**, 9697–9707.
10 D. O. De Haan, M. A. Tolbert and J. L. Jimenez, *Geophys. Res. Lett.*, 2009, **36**, L11819, DOI: 10.1029/12009gl037441.
11 A. Gelencser, A. Hoffer, G. Kiss, E. Tombacz, R. Kurdi and L. Bencze, *J. Atmos. Chem.*, 2003, **45**, 25–33.
12 A. Hoffer, G. Kiss, M. Blazso and A. Gelencser, *Geophys. Res. Lett.*, 2004, **31**, L06115, DOI: 10.1029/2003GL018962.
13 J. L. Chang and J. E. Thompson, *Atmos. Environ.*, 2010, **44**, 541–551.
14 H. E. Krizner, D. O. De Haan and J. Kua, *J. Phys. Chem. A*, 2009, **113**, 6994–7001.
15 B. Noziere and W. Esteve, *Atmos. Environ.*, 2007, **41**, 1150–1163.
16 M. T. Casale, A. R. Richman, M. J. Elrod, R. M. Garland, M. R. Beaver and M. A. Tolbert, *Atmos. Environ.*, 2007, **41**, 6212–6224.
17 B. Noziere, D. Voisin, C. A. Longfellow, H. Friedli, B. E. Henry and D. R. Hanson, *J. Phys. Chem. A*, 2006, **110**, 2387–2395.
18 J. Zhao, N. P. Levitt and R. Zhang, *Geophys. Res. Lett.*, 2005, **32**, L09802, DOI: 10.1029/2004GL022200.

19 B. Noziere and W. Esteve, *Geophys. Res. Lett.*, 2005, **32**, L03812, DOI: 10.1029/2004GL021942.
20 W. Esteve and B. Noziere, *J. Phys. Chem. A*, 2005, **109**, 10920–10928.
21 R. M. Garland, M. J. Elrod, K. Kincaid, M. R. Beaver, J. L. Jimenez and M. A. Tolbert, *Atmos. Environ.*, 2006, **40**, 6863–6878.
22 M. Z. Jacobson, *J. Geophys. Res.*, 1999, **104**, 3527–3542.
23 J. N. Pitts, Jr., K. A. Van Cauwenberghe, D. Grosjean, J. P. Schmid, D. R. Fitz, W. L. Belser, Jr., G. B. Knudson and P. M. Hynds, *Science*, 1978, **202**(4367), 515–519.
24 N. O. A. Kwamena and J. P. D. Abbatt, *Atmos. Environ.*, 2008, **42**, 8309–8314.
25 J. Laskin, A. Laskin, P. J. Roach, G. W. Slysz, G. A. Anderson, S. A. Nizkorodov, D. L. Bones and L. Q. Nguyen, *Anal. Chem.*, 2010, **82**, 2048–2058.
26 D. L. Bones, D. K. Henricksen, S. A. Mang, M. Gonsior, A. P. Bateman, T. B. Nguyen, W. J. Cooper and S. A. Nizkorodov, *J. Geophys. Res.*, 2010, **115**, D05203, DOI: 10.1029/2009jd012864.
27 K. M. Updyke, T. B. Nguyen, sa. S. A. and sa. Nizkorodov, *Atmos. Environ.*, 2012, **63**, 22–31.
28 C. Geron, R. Rasmussen, R. R. Arnts and A. Guenther, *Atmos. Environ.*, 2000, **34**, 1761–1781.
29 S. K. Brown, M. R. Sim, M. J. Abramson and C. N. Gray, *Indoor Air*, 1994, **4**, 123–134.
30 S. Leungsakul, M. Jaoui and R. M. Kamens, *Environ. Sci. Technol.*, 2005, **39**, 9583–9594.
31 H. Hakola, J. Arey, S. M. Aschmann and R. Atkinson, *J. Atmos. Chem.*, 1994, **18**, 75–102.
32 H. Debus, *Justus Liebigs Ann. Chem.*, 1858, **107**, 199–208.
33 G. Yu, A. R. Bayer, M. M. Galloway, K. J. Korshavn, C. G. Fry and F. N. Keutsch, *Environ. Sci. Technol.*, 2011, **45**, 6336–6342.
34 D. O. De Haan, L. N. Hawkins, J. A. Kononenko, J. J. Turley, A. L. Corrigan, M. A. Tolbert and J. L. Jimenez, *Environ. Sci. Technol.*, 2011, **45**, 984–991.
35 T. B. Nguyen, P. B. Lee, K. M. Updyke, D. L. Bones, J. Laskin, A. Laskin and S. A. Nizkorodov, *J. Geophys. Res.*, 2012, **117**, D01207, DOI: 10.1029/2011JD016944.
36 T. Berndt, O. Boge and F. Stratmann, *Atmos. Environ.*, 2003, **37**, 3933–3945.
37 M. L. Walser, Y. Desyaterik, J. Laskin, A. Laskin and S. A. Nizkorodov, *Phys. Chem. Chem. Phys.*, 2008, **10**, 1009–1022.
38 B. R. Larsen, M. Lahaniati, A. Calogirou and D. Kotzias, *Chemosphere*, 1998, **37**, 1207–1220.
39 D. Johnson and G. Marston, *Chem. Soc. Rev.*, 2008, **37**, 699–716.
40 Y. Ma, A. T. Russell and G. Marston, *Phys. Chem. Chem. Phys.*, 2008, **10**, 4294–4312.
41 C. M. Binder, D. D. Dixon, E. Almaraz, M. A. Tius and B. Singaram, *Tetrahedron Lett.*, 2008, **49**, 2764–2767.
42 K. Griesbaum, Y. Dong and K. J. McCullough, *J. Org. Chem.*, 1997, **62**, 6129–6136.
43 C. W. Dicus, D. Willenbring and M. H. Nantz, *J. Labelled Compd. Radiopharm.*, 2005, **48**, 223–229.
44 S.-T. Liu, K. V. Reddy and R.-Y. Lai, *Tetrahedron*, 2007, **63**, 1821–1825.
45 D. Yang and C. Zhang, *J. Org. Chem.*, 2001, **66**, 4814–4818.
46 H. E. Gottlieb, V. Kotlyar and A. Nudelman, *J. Org. Chem.*, 1997, **62**, 7512–7515.
47 Y. Chen and T. C. Bond, *Atmos. Chem. Phys.*, 2010, **10**, 1773–1787.
48 S. L. Clegg, P. Brimblecombe and A. S. Wexler, *J. Phys. Chem. A*, 1998, **102**, 2137–2154.
49 T. B. Nguyen, A. P. Bateman, D. L. Bones, S. A. Nizkorodov, J. Laskin and A. Laskin, *Atmos. Environ.*, 2010, **44**, 1032–1042.
50 T. B. Nguyen, J. Laskin, A. Laskin and S. A. Nizkorodov, *Environ. Sci. Technol.*, 2011, **45**, 6908–6918.
51 L. F. H. Bovey, *J. Opt. Soc. Am.*, 1951, **41**, 836–848.
52 Y. Futami, Y. Ozaki, Y. Hamada, M. J. Wojcik and Y. Ozaki, *Chem. Phys. Lett.*, 2009, **482**, 320–324.
53 I. V. Rubtsov, K. Kumar and R. M. Hochstrasser, *Chem. Phys. Lett.*, 2005, **402**, 439–443.
54 E. L. Saier, L. R. Cousins and M. R. Basila, *J. Phys. Chem.*, 1962, **66**, 232–235.
55 G. Socrates, *Infrared and Raman Characteristic Group Frequencies*, John Wiley and Sons, Ltd., Chichester, 3rd edn, 2001.
56 R. D. Bicca Alencastro, S. Badilescu, L. S. Lussier, C. Sandorfy, H. L. Thanh and D. Vocelle, *Int. J. Quantum Chem.*, 1990, **38**, 173–179.
57 K. J. Rothschild, P. Roepe, J. Lugtenburg and J. A. Pardoen, *Biochemistry*, 1984, **23**, 6103–6109.
58 H. Kato, O. Nishikawa, T. Matsui, S. Honma and H. Kokado, *J. Phys. Chem.*, 1991, **95**, 6014–6016.
59 E. Zhukovsky and D. Oprian, *Science*, 1989, **246**, 928–930.
60 P. Dziedzic, A. Bartoszewicz and A. Córdova, *Tetrahedron Lett.*, 2009, **50**, 7242–7245.
61 T. W. G. Solomons and C. B. Fryhle, *Organic Chemistry*, John Wiley & Sons, Inc., Hoboken, NJ, 8th edn, 2004.

62 J. W. Wijnen and J. B. Engberts, *Liebigs Ann./Recl.*, 1997, 1085–1088.
63 P. A. Grieco, D. T. Parker, M. Cornwell and R. Ruckle, *J. Am. Chem. Soc.*, 1987, **109**, 5859–5861.
64 J. W. Wijnen and J. B. F. N. Engberts, *J. Org. Chem.*, 1997, **62**, 2039–2044.
65 A. Laskin, J. S. Smith and J. Laskin, *Environ. Sci. Technol.*, 2009, **43**, 3764–3771.
66 B. Plietker, *Tetrahedron: Asymmetry*, 2005, **16**, 3453–3459.
67 R. Howe and F. J. McQuillin, *J. Chem. Soc.*, 1958, 1513–1518.
68 V. Amarnath, D. C. Anthony, K. Amarnath, W. M. Valentine, L. A. Wetterau and D. G. Graham, *J. Org. Chem.*, 1991, **56**, 6924–6931.
69 L. Carlton, B. Staskun and T. van Es, *Magn. Reson. Chem.*, 2006, **44**, 510–514.
70 C. Mukhopadhyay, A. Datta and R. J. Butcher, *Tetrahedron Lett.*, 2009, **50**, 4246–4250.
71 Q.-X. Guo, H. Liu, C. Guo, S.-W. Luo, Y. Gu and L.-Z. Gong, *J. Am. Chem. Soc.*, 2007, **129**, 3790–3791.
72 J. L. Hogg, D. A. Jencks and W. P. Jencks, *J. Am. Chem. Soc.*, 1977, **99**, 4772–4778.
73 P. S. Tobias and R. G. Kallen, *J. Am. Chem. Soc.*, 1975, **97**, 6530–6539.
74 C.-H. Jun, C. W. Moon and D.-Y. Lee, *Chem.–Eur. J.*, 2002, **8**, 2422–2428.
75 R. S. Becker and K. Freedman, *J. Am. Chem. Soc.*, 1985, **107**, 1477–1485.
76 H. Akita, S. P. Tanis, M. Adams, V. Balogh-Nair and K. Nakanishi, *J. Am. Chem. Soc.*, 1980, **102**, 6370–6372.
77 C. Paal, *Ber. Dtsch. Chem. Ges.*, 1884, **17**, 2756–2767.
78 L. Knorr, *Ber. Dtsch. Chem. Ges.*, 1884, **17**, 2863–2870.
79 C. P. Schwartz, J. S. Uejio, A. M. Duffin, A. H. England, D. Prendergast and R. J. Saykally, *J. Chem. Phys.*, 2009, **131**, 114509–114508.
80 J. Y. Lee, D. Y. Kim and C. Y. Kim, *Synth. Met.*, 1995, **74**, 103–106.
81 W. Wang, D. Yu and F. Tian, *Synth. Met.*, 2008, **158**, 717–721.
82 K. Kijewska, P. Głowala, K. Wiktorska, M. Pisarek, J. Stolarski, D. Kępińska, M. Gniadek and M. Mazur, *Polymer*, 2012, **53**, 5320–5329.
83 D. Birnbaum and B. E. Kohler, *J. Chem. Phys.*, 1991, **95**, 4783–4789.

